Dissipative Solitary States in Driven Surface Waves

O. Lioubashevski, H. Arbell, and J. Fineberg
The Racah Institute of Physics, The Hebrew University of Jerusalem, Jerusalem 91904, Israel
(Received 4 January 1996)

We present an experimental study of highly localized, solitonlike structures that propagate on the two-dimensional surface of highly dissipative fluids. Like the well-known Faraday instability, these highly dissipative structures are driven by means of the spatially uniform, vertical acceleration of a thin fluid layer. These structures, harmonically coupled to the external driving frequency, are observed above a critical ratio of the viscous boundary layer height to the depth of the fluid layer for a wide range of fluid viscosities and system parameters. [S0031-9007(96)00186-X]

PACS numbers: 47.20.Gv, 47.20.Ky, 47.35.–i, 47.54.+r

Driven nonlinear systems have been the subject of substantial interest over the past decade. A large class of such systems, at a critical driving amplitude, bifurcate from an initial featureless state to a global state characterized by a well-defined mode or pattern which retains a certain symmetry of the system. As the driving is increased, the initial pattern may become unstable, undergoing additional bifurcations which further reduce the system's symmetry. Dissipation in these systems is not confined to a single region but, following the pattern, is uniformly distributed throughout the medium.

Uniformly distributed patterns are not the only types of structures that arise in driven nonlinear systems. In two or three spatial dimensions (2D or 3D), long-lived, localized modes such as vortices [1] in turbulent systems or spiral waves in pattern-forming systems [2] appear to be widespread in driven dissipative systems. Localized, solitonlike structures, ubiquitous in nonlinear conservative systems, are rarely if at all observed [3] in highly dissipative 2D or 3D systems. In this paper, we observe the appearance of such states in the well-known pattern-forming system generally used in studies of the Faraday instability. As the system becomes highly dissipative, it undergoes a sharp transition from one of states characterized by global patterns to one of highly localized, propagating, particlelike states. These states raise the intriguing question of why, when sufficiently dissipative, will a system prefer to *localize* rather than uniformly distribute its dissipation.

Our experimental system consists of a thin, horizontal (normal to gravity), 2D fluid layer subjected to uniform, externally imposed oscillations in the vertical (parallel to gravity) direction. The acceleration amplitude a of the fluid layer can be viewed as the system's control parameter. At a critical value a_c the initial spatially uniform fluid state loses its stability. The system is further characterized by the quantities ω, h, ν, ρ, and σ defined as the externally imposed angular frequency, fluid depth, kinematic viscosity, fluid density, and surface tension, respectively. As a pattern-forming system, this system has been widely studied with most previous experiments performed in the regime of large fluid depth ($\lambda \ll h$ where λ is the wavelength of the pattern excited on the fluid surface) and low dissipation (where the dissipation rate $\sim \nu/\lambda^2 \ll \omega$). These studies include nonlinear mode interactions [4] in small aspect ratio (defined as the ratio between the horizontal size of the system and λ) systems where the excited modes are well separated and the dynamics and disorder of patterns [5] in larger aspect ratio systems.

Recent work [6,7] has shown the utility of using more highly dissipative fluids to reduce mode quantization effects due to the lateral boundaries together with relatively thin fluid layers ($h < \lambda$) to damp out long wavelength modes (for a detailed discussion see [6b]). Linear stability analysis for finite h and ν has recently [8] yielded predictions for a_c and λ that match experiments [7] for the high ν, shallow fluid layer regime.

An important parameter in this system is the size of the viscous boundary layer $\delta \equiv (\nu/\omega)^{1/2}$. We view a highly dissipative system as one where the characteristic time for dissipation h^2/ν is on the order of the driving period $1/\omega$. In this region δ is on the order of h. The ratio δ/h (or, equivalently, the ratio between the forcing and dissipative time scales) will turn out to be critical for the selection of the fluid state. The work described here was performed for larger values of δ/h ($0.15 < \delta/h < 1.2$) than in previous experiments [6,7] ($0.03 < \delta/h < 0.27$) on viscous fluids and thin fluid layers.

In our experiments we used a 144.0 mm diameter circular cell where the fluid rests on an aluminum plate, diamond machined to a flatness of better than 1 μm and polished to a mirror surface. The cell's lateral boundaries were made of Delrin with, as in [7], walls sloped at a 20° angle to reduce meniscus formation on the fluid surface. Although a variety of fluids were used, most of our quantitative results were obtained using a hydrocarbon flushing fluid [9], TKO-FF, with $1.0 < h < 3.0$ mm. This nonhygroscopic, Newtonian fluid has a low vapor pressure (1×10^{-5} torr @ 25 °C) enabling us to work with the fluid exposed to air. The temperature was regulated to within 0.01 °C by IR lamps controlled by a temperature probe imbedded in the bottom plate. By adjusting the working temperature of the fluid, σ varies [10] between 29.6 and 31.0 dyn/cm and ν was varied from 1.7 to 0.4 St between 20 and 45 °C.

The working cell was mounted on a mechanical shaker (Unholtz-Dickie 5PM) providing vertical acceleration from 0 to 30gs. The range of driving frequencies used (20–80 Hz) was limited by its maximum output (225 Nt) and stroke (12.5 mm). The acceleration, regulated to within 0.01g, was monitored by a calibrated accelerometer (Bruel & Kajer 4394) mounted on the cell. Visualization of the system from above was performed by shadowgraph and from the side by the scattering of a diffuse backlight by the fluid. Because of its high sensitivity to minute curvature of the fluid surface, shadowgraph visualization was used to determine the onset of instability [11]. The side visualization was used for the quantitative study of high amplitude states. Both methods used stroboscopic lighting (1 μs illumination time) with variable period and phase relative to the driving.

The primary bifurcation to a spatially confined pattern ("confined state"), shown in Fig. 1, was observed throughout the entire parameter space. This state, composed of spatially stationary standing waves, had been seen previously, but its localized nature was ascribed to apparatus inhomogeneities [12]. Our observations indicate that this subharmonic state is intrinsic to the system and not a boundary effect, as this state can appear in either the cell's center or sides. The state can be pinned by small nonuniformities in the cell or fluid depth; a 0.2 mrad shift in the leveling of the apparatus is sufficient to shift its position.

As a is increased past a_c, the confined state loses stability in one of three scenarios. For low values of δ/h the system will bifurcate to a subharmonic global pattern similar to those observed in previous work [6,7], intermediate values of δ/h lead to a subharmonic ringlike standing wave encompassing the circumference of the cell, and large values of δ/h give rise to the propagating solitary structures that are the subject of this Letter [13].

Photographs of a typical propagating solitary structure are displayed in Fig. 2. Whereas the stationary states observed are composed of subharmonic standing waves which oscillate at an angular frequency of $\omega/2$, these solitary states (SS) are harmonic [14] with the driving, as their structure repeats itself with a basic period of $2\pi/\omega$. The 3D structure of the states shown in the figure is representative; their basic structure is independent of the driving frequency, fluid parameters, or, to a large degree, the driving acceleration. At a well-defined value of a, these states bifurcate with a large and finite initial amplitude. Their vertical amplitude is not strongly dependent on a and is typically an order of magnitude larger than h. The width in the propagation direction of the fingerlike structures seen in Fig. 2 is extremely small ($<h$). Increasing the driving amplitude leads to increased spontaneous formation of these states with necking and eventual drop ejection at high driving amplitudes [15].

The characteristic profiles of SS, photographed normal to their propagation direction at a single phase relative to the driving signal, are shown in Fig. 3. Their horizontal size scales as $(1.34 \pm 0.04)\lambda$. These states are stable and single SS have been observed to circle the cell perimeter for thousands of driving periods until experimental conditions are changed. The main mechanism for their destruction is by collision with either other SS or the lateral boundaries. The existence of these states is not due to the lateral boundary of the system. Generated by either collisions or external perturbations to the system, they can exist far from the system boundaries, as Fig. 2 shows, with no apparent difference in form or properties relative to states that propagate adjacent to the cell boundaries.

The onset of the solitary structures occurs in the near vicinity of a_c. In the phase diagram in Fig. 4 we compare

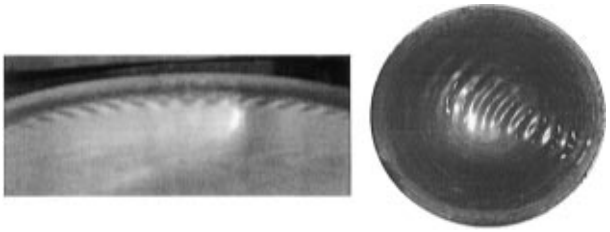

FIG. 1. View of the spatially confined, primary instability (right) from above via shadowgraph visualization when the pattern was observed in the center of the cell $\omega/2\pi = 36$ Hz, $\nu = 1.25$ St, $h = 2.1$ mm (left) from the side with the pattern confined near the lateral boundary of the cell, $\omega/2\pi = 42$ Hz, $\nu = 0.63$ St, $h = 1.0$ mm.

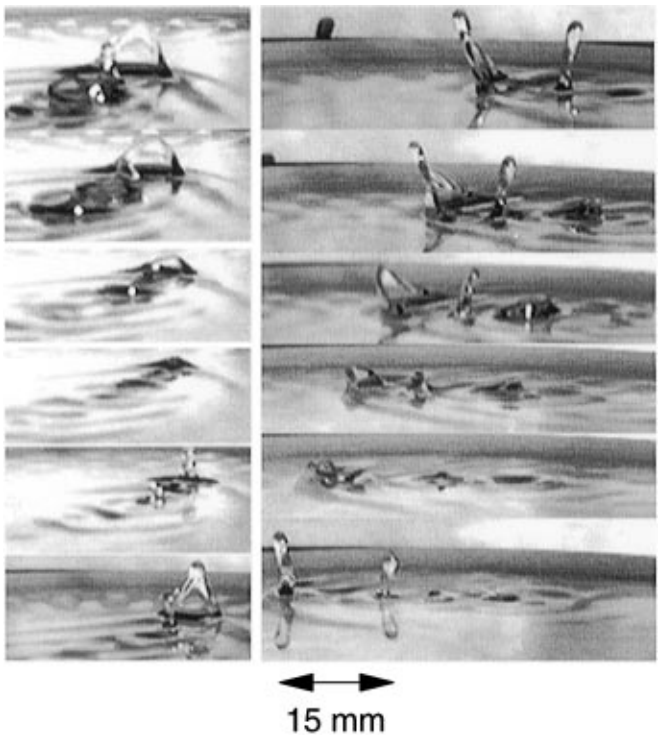

FIG. 2. Typical propagating solitary states visualized from the side. The system was driven at 41 Hz, $\nu = 0.86$ St, $h = 1.3$ mm, and visualized at 20 msec intervals. The spatial form of these states changes harmonically with the driving. One repetition period of states propagating from right to left (right side) and away from the camera (left side) is shown.

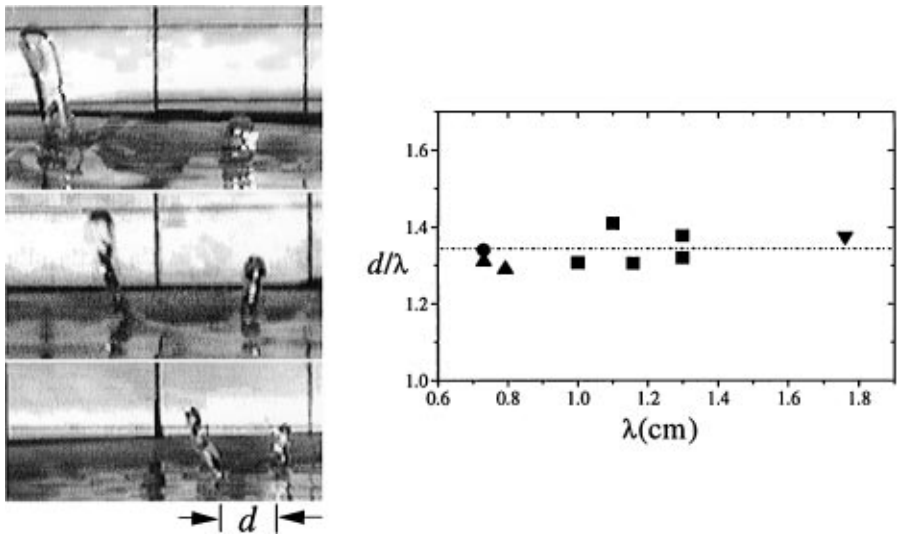

FIG. 3. Scaling of the solitary state. (Left) Transverse views of the solitary states $\omega/2\pi = 20$ Hz, $\nu = 1.4$ St, $h = 2.9$ mm (top), $\omega/2\pi = 26$ Hz, $\nu = 1.25$ St, $h = 2.1$ mm (center), and $\omega/2\pi = 41$ Hz, $\nu = 0.86$ St, $h = 1.0$ mm (lower). (Right) d/λ vs the wavelength λ of the *primary* pattern, where d (see figure) is the distance between the fingerlike structures composing the solitary state. The dotted line indicates the mean value of $d/\lambda = 1.34$.

the acceleration threshold values [16] of the SS with those of the global patterns for different values of ν and ω. Defining $\varepsilon \equiv (a - a_c)/a_c$ we see that, for a given fluid depth, the threshold values of ε, as a function of ω, coincide for fluids of different ν for both the SS and patterns. The (lower) SS branch does *not* exist for low ν although the global patterns (upper branch) are unperturbed, occurring at the same values of ε as the higher viscosity states (the SS observed in Fig. 4, *above* the global patterns correspond to the transition region). This indicates that the global states cannot be viewed as a secondary instability of the SS. At the instability threshold for the global patterns, a region of coexistence of the two states is observed. The bifurcation to the solitary branch from the (primary) confined state displays a large degree of hysteresis (>10%) indicating a first order transition. For sufficiently large perturbations (e.g., mechanically striking the fluid layer) SS can be excited prior to the onset of the confined pattern.

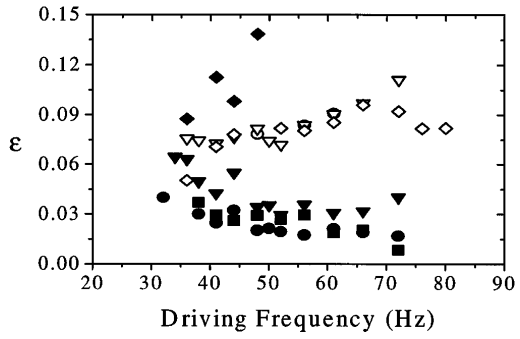

FIG. 4. Phase diagram of the solitary states (lower branch) and global patterns (upper branch) as a function of the driving frequency $\omega/2\pi$. $\varepsilon \equiv (a - a_c)/a_c$, where a_c is the critical driving acceleration of the primary instability. The data were all for $h = 1.3$ mm with fluid viscosities of 0.86 St (□), 0.74 St (▽), 0.63 St (○), and 0.52 St (◇). Solid symbols represent solitary states and open symbols represent patterns.

How general are these SS and why have they not been observed in previous experiments? The disappearance of the SS branch at lower viscosities, observed in Fig. 4, indicates the importance of dissipation on the stability of the SS. Over the entire range of ν, h, and ω used, no SS are observed above a critical value of ω. A dimensionless number relating these quantities is the ratio of the boundary layer thickness δ to h. Plotting δ/h as a function of ω [Fig. 5(a)], we observe that below a critical value $(\delta/h)_{\text{crit}}$ (dashed line), SS will give way to the global patterns observed in previous studies. In Fig. 5(b) we show that $(\delta/h)_{\text{crit}}$ is indeed constant for a variety of fluid viscosities and depths. The critical value $(\delta/h)_{\text{crit}} = 0.30$ explains why SS were not observed in previous experiments where $\delta/h < 0.27$.

The parameter $(\delta/h)^{-2}$ can be viewed as analogous to a Reynolds number of the flow. This is seen by scaling [17] the externally forced Navier-Stokes equations by the length scale h, the time scale ω^{-1}. $(\delta/h)_{\text{crit}}$ occurs in the region where the forced oscillation of the fluid surface approaches critical damping (when the viscous and driving time scales are comparable or, equivalently, δ approaches h). This indicates that the SS are crucially linked to the system dissipation. In this regime, the symmetry between upward and downward perturbations of the fluid surface is broken as the fluid surface "feels" the lower boundary. This up-down symmetry breaking may play an essential role in the creation of these highly asymmetric states. The value of $(\delta/h)_{\text{crit}}$ underlines the qualitative difference between the dissipative SS observed here and "trough" solitons [18]. These, described by a nonlinear Schrödinger equation, were observed in a nearly conservative, 1D system for $\delta/h \sim 0.01$, a value far below $(\delta/h)_{\text{crit}}$.

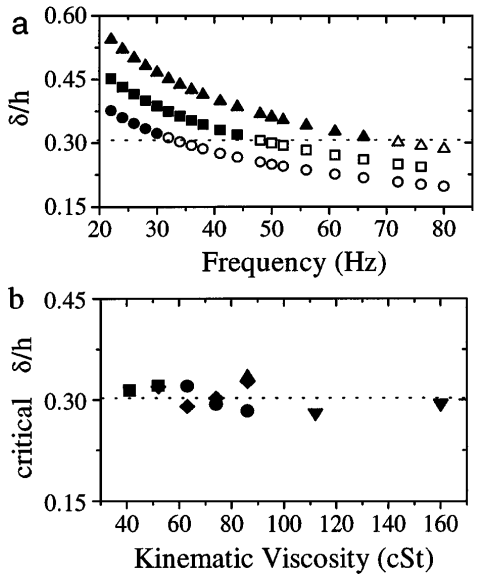

FIG. 5. (a) Boundary layer thickness to fluid depth ratios δ/h observed for solitary states (solid symbols) and global patterns (open symbols): ○ $h = 2.1$ mm, $\nu = 0.86$ St; □ $h = 1.5$ mm, $\nu = 0.63$ St; and ◇ $h = 1.0$ mm, $\nu = 0.41$ St. Note the value $(\delta/h)_{\text{crit}} = 0.30$ (dashed line) at which the transition between states occurs. (b) $(\delta/h)_{\text{crit}}$ as a function of fluid viscosity for fluid depths of 1.0 mm (□), 1.3 mm (○), 1.5 mm (◇), and 2.1 mm (▽).

Although a detailed description [19] is beyond the scope of this Letter, we will briefly mention a few interesting properties of SS. Unlike many types of solitary structures (e.g., Korteweg–de Vries solitons whose propagation velocity is amplitude dependent or nonlinear Schrödinger equation solitons whose propagation velocity can vary) we observe no dependence of their propagation velocity V on either the amplitude of the state or a. V is steady with a constant value for a given value of ω. The scale of V is that of the group velocity of linear surface waves but with a different ω dependence. Unlike classic solitons, whose interaction results in a simple phase change, SS, upon colliding, appear particlelike and can either mutually annihilate, pass through each other with a slight loss of amplitude, or "collide" to create a new state whose direction of propagation is at an angle to that of the original states. In addition to single SS, "multiple-particle" bound states have been observed.

In conclusion, we have observed a novel, highly localized fluid state which exists *solely* when the system is sufficiently dissipative. It remains a challenge to find a theoretical description of both the existence and selection of this state together with the nonlinear mechanism responsible for its localization.

The authors wish to acknowledge the support of the Wolfson family charitable trust (Grant No. 43/93-2). We also would like to thank W. S. Edwards, B. Meerson, L. S. Tuckerman, G. Cohen, and C. Cohen for stimulating conversations and invaluable advice.

[1] J. Sommeria, S. D. Meyers, and H. L. Swinney, Nature (London) **331**, 689 (1988); Z-S. She, E. Jackson, and S. A. Orszag, Proc. R. Soc. London A **434**, 101 (1991).

[2] See, e.g., W. Y. Tam, W. Horsthemke, Z. Noszticzius, and H. L. Swinney, J. Chem. Phys. **188**, 3395 (1988); E. Bodenschatz, J. R. DeBruyn, D. S. Cannell, and G. Ahlers, Phys. Rev. Lett. **71**, 2026 (1993).

[3] Possible candidates are localized states in the convection of binary fluid mixtures in 2D [see V. Steinberg, J. Fineberg, E. Moses, and I. Rehberg, Physica (Amsterdam) **37D**, 359 (1989) and K. Lerman, E. Bodenschatz, D. S. Cannell, and G. Ahlers, Phys. Rev. Lett. **70**, 3572 (1993)] and in a flowing viscous film [V. I. Petviashvilli and O. Y. Tsevelodub, Sov. Phys. Dokl. **23**, 117 (1978)].

[4] See, e.g., J. P. Gollub and C. W. Meyer, Physica (Amsterdam) **6D**, 337 (1983); J. P. Gollub and S. Ciliberto, Phys. Rev. Lett. **52**, 922 (1984); F. Simonella and J. P. Gollub, J. Fluid Mech. **199**, 471 (1989).

[5] See, e.g., A. B. Ezerskii, P. I. Korotin, and M. I. Rabinovich, Sov. Phys. JETP **41**, 157 (1986); N. B. Tufillaro, R. Ramshankar, and J. P. Gollub, Phys. Rev. Lett. **62**, 422 (1989); S. Ciliberto, S. Douady, and S. Fauve, Europhys. Lett. **15**, 23 (1991); B. Christiansen, P. Alstrom, and M. Levinsen, Phys. Rev. Lett. **68**, 2157 (1992); E. Bosch and W. van der Water, Phys. Rev. Lett. **70**, 3420 (1993).

[6] (a) W. S. Edwards and S. Fauve, Phys. Rev. E **47**, 788 (1993); (b) J. Fluid Mech. **278**, 123 (1994).

[7] J. Bechhoefer, V. Ego, S. Manneville, and B. Johnson, J. Fluid Mech. **288**, 325 (1995).

[8] K. Kumar and L. S. Tuckerman, J. Fluid Mech. **279**, 49 (1994).

[9] The fluid is obtainable from the Kurt J. Lesker Co.

[10] σ is fit well by $\sigma = 33.2 - 0.117T + 7 \times 10^{-4}T^2$ where T is the temperature in °C.

[11] At the frequencies used, deflections on the order of 10 μm of the fluid surface can be detected by shadowgraph.

[12] T. Besson, W. S. Edwards, J. P. Gollub, and L. S. Tuckerman, report, 1995 (to be published).

[13] The initial confined, global, and ringlike states will be described in a subsequent publication.

[14] At high amplitudes, the repetition frequency is slightly different than ω, conceivably due to nonlinear detuning effects. These states might be related to harmonic *linear* states predicted for small values of h. See K. Kumar, Proc. R. Soc. London (to be published).

[15] See C. L. Goodridge, W. T. Shi, and D. P. Lathrop, Phys. Rev. Lett. **76**, 1828 (1996).

[16] The data presented, for given experimental conditions, were entirely reproducible. Minute changes in the apparatus leveling and/or the fluid depth, however, can cause measurable shifts in the measured values of a_c.

[17] Additional dimensionless parameters in this scaling are the ratio between the forcing amplitude a/ω^2 and h as well as λ/h and the ratio of the effective capillary length $(\sigma/\rho a)^{1/2}$ and δ.

[18] J. Wu, R. Keolian, and I. Rudnick, Phys. Rev. Lett. **52**, 1421 (1984); A. Larraza and S. Putterman, J. Fluid Mech. **148**, 443 (1984); J. W. Miles, J. Fluid Mech. **148**, 451 (1984).

[19] O. Lioubashevsky, H. Arbel, and J. Fineberg (to be published).